



# Massless Neutrino Oscillation via Maximally Natural Vacuum Wavefunctions\*

Peter Cameron – Brookhaven National Laboratory (retired) electronGaugeGroup@gmail.com



**Abstract:** Two essential conceptual structures - geometric representation of Clifford algebra wavefunctions [1,2] and quantized impedances of wavefunction interactions [3] - are absent from particle theorists' toolkits. Their synthesis offers a complementary Standard Model perspective, focusing not on Lagrangian flow of energy and information, but rather on what governs amplitude and phase of that flow - impedance matching of wavefunction interactions. Photon excitation of two-component Dirac spinor vacuum wavefunctions permits calculation of two fundamental constants - electric permittivity and magnetic permeability - and from these the scale-invariant 377 ohm far-field vacuum impedance excited and seen by the photon [4,5,6]. This suggests extending the method to near-field of the full eight-component geometric vacuum wavefunction of Clifford algebra [7]. Such a model offers maximally natural three-component massless neutrino oscillation via the additional vacuum impedance phase shifts [8], with absence of right-hand neutrinos required by failure of three-component associativity in the eight-component octonion algebra [9].

## 1. Geometric Representation of Clifford Algebra

In Geometric Algebra, Pauli matrices are basis vectors of space, Dirac matrices those of spacetime. The SU(2) Pauli algebra is the double cover of SO(3), the algebra of 3D Euclidian space. The minimally complete algebra is comprised of one scalar point, three vector line elements (three orientational degrees of freedom), three bivector area elements, and one trivector volume element. They comprise a maximally natural vacuum wavefunction.

Wavefunction interactions are modeled by the geometric product of Clifford algebra, multiplying not numbers or symbols but geometric objects, changing 'grades' (dimensionality), making GA unique in the ability to handle dynamics in all dimensions. The product turns fermions into bosons, bosons into fermions. Dynamic supersymmetry emerges naturally from interactions, as does time in the grade increase from 3D space to 6D phase space generated by wedge products [10]. The "...problem is that even though we can transform the line continuously into a point, we cannot undo this transformation and have a function from the point back onto the line..." [11].

Grade increasing operations break topological symmetry, with the exception of wedge products of scalars. Scalars are point objects having no spatial dimensionality, cannot raise grades. This is of particular interest for the *Higgs*.

Given two vectors  $W$  and  $Z$ , the geometric product  $WZ$  changes grades. In the product  $WZ = W \cdot Z + W \wedge Z$ , two grade 1 vector bosons transform into a grade 0 scalar boson and grade 2 bivector fermion,  $WZ = Higgs + top$ .

Symmetry breaking of wedge product manifests in the appearance of spin  $\frac{1}{2}$  *top* from the product of two bosons. Sum of  $W$  and  $Z$  masses equals *top* at  $<1\%$ , difference is  $\sim 10.8$  GeV/c<sup>2</sup>, relevant to the 10 GeV coherence length of figure 4. The four superheavies comprise a minimally complete 2D Clifford algebra - one scalar, two vectors, and one bivector.

electric charge	elec dipole moment 1	elec dipole moment 2	mag flux quantum	elec flux quantum 1	elec flux quantum 2	magnetic moment	magnetic charge
$e$	$d_{E1}$	$d_{E2}$	$\phi_B$	$\phi_{E1}$	$\phi_{E2}$	$\mu_{Bohr}$	$g$
scalar	vector	vector	bivector	bivector	bivector	bivector	trivector
$ee$	$ed_{E1}$	$ed_{E2}$	$e\phi_B$	$e\phi_{E1}$	$e\phi_{E2}$	$e\mu_B$	$eg$
scalar	vector	vector	bivector	bivector	bivector	bivector	trivector
$d_{E1}e$	$d_{E1}d_{E1}$	$d_{E1}d_{E2}$	$d_{E1}\phi_B$	$d_{E1}\phi_{E1}$	$d_{E1}\phi_{E2}$	$d_{E1}\mu_B$	$d_{E1}g$
vector	bivector	bivector	bivector	bivector	bivector	bivector	bivector
$d_{E2}e$	$d_{E2}d_{E1}$	$d_{E2}d_{E2}$	$d_{E2}\phi_B$	$d_{E2}\phi_{E1}$	$d_{E2}\phi_{E2}$	$d_{E2}\mu_B$	$d_{E2}g$
vector	bivector	bivector	bivector	bivector	bivector	bivector	bivector
$\phi_B e$	$\phi_B d_{E1}$	$\phi_B d_{E2}$	$\phi_B \phi_B$	$\phi_B \phi_{E1}$	$\phi_B \phi_{E2}$	$\phi_B \mu_B$	$\phi_B g$
bivector	bivector	bivector	scalar + bivector	bivector + trivector	bivector + trivector	bivector	bivector
$\phi_{E1} e$	$\phi_{E1} d_{E1}$	$\phi_{E1} d_{E2}$	$\phi_{E1} \phi_B$	$\phi_{E1} \phi_{E1}$	$\phi_{E1} \phi_{E2}$	$\phi_{E1} \mu_B$	$\phi_{E1} g$
bivector	bivector	bivector	bivector	bivector	bivector	bivector	bivector
$\phi_{E2} e$	$\phi_{E2} d_{E1}$	$\phi_{E2} d_{E2}$	$\phi_{E2} \phi_B$	$\phi_{E2} \phi_{E1}$	$\phi_{E2} \phi_{E2}$	$\phi_{E2} \mu_B$	$\phi_{E2} g$
bivector	bivector	bivector	bivector	bivector	bivector	bivector	bivector
$\mu_B e$	$\mu_B d_{E1}$	$\mu_B d_{E2}$	$\mu_B \phi_B$	$\mu_B \phi_{E1}$	$\mu_B \phi_{E2}$	$\mu_B \mu_B$	$\mu_B g$
bivector	bivector	bivector	bivector	bivector	bivector	bivector	bivector
$g e$	$gd_{E1}$	$gd_{E2}$	$g\phi_B$	$g\phi_{E1}$	$g\phi_{E2}$	$g\mu_B$	$gg$
trivector	bivector + quadvector	bivector + quadvector	bivector	bivector + pentavector	bivector + pentavector	bivector	scalar + sv

**Fig. 2** Impedance representation of the S-matrix, generated by Clifford products of octonion wavefunctions at top and left. As with the two spinors of the Dirac wavefunction (circled in blue), opposite sides of main diagonal are particle and antiparticle, rotating in opposite directions in phase space. Modes of the three-component neutrino wavefunction  $\phi_B \phi_{E1} g$  are indicated by ellipses. Mode impedances indicated by symbols (triangle, diamond,...) are plotted in figure 4.

Vacuum wavefunction physical manifestation follows from introduction of the electromagnetic coupling constant  $\alpha = e^2/4\pi\epsilon_0\hbar c$ . Combinations of the four fundamental constants that define  $\alpha$  permit assigning topologically appropriate quantized E and B fields to the eight fundamental geometric objects that comprise the vacuum wavefunction, as shown at top and left of figure 2 [e8?]. Given that fields of quantum field theory are quantized, it is unavoidable that impedances of geometric wavefunction interactions will likewise be quantized [3]. **This is important** - impedance matching governs amplitude and phase of energy/information transmission.

## 2. Impedance Quantization

Impedances are of two types, scale dependent and scale invariant. Invariant impedances are *topological*, include quantum Hall and Aharonov-Bohm of the vector Lorentz force, centrifugal, chiral, Coriolis, and three body, correspond to  $1/r^2$  potentials of rotation gauge fields. They cannot be shielded, are both causal and acausal, agents of both local and non-local entanglement. They can do no work - resultant direction of motion is perpendicular to applied force - communicate only phase, not a single measurement observable.

Scale dependent impedances are *geometric*, include Coulomb, dipole, scalar Lorentz,... correspond to translation gauge fields, the  $1/r$  and  $1/r^3$  potentials of monopole and dipole interactions. They can be shielded, are causal agents of local entanglement, regulate both amplitude and phase.

Photon appears unique, possessing both scale dependent near-field and invariant far-field impedances.

### Hydrogen Atom Ionization

Figure 3 shows a 13.6 eV photon entering from right at the 377 ohm far-field impedance. Encountering a 'bound' electron at scale of the inverse Rydberg, it excites dipole modes, the opposing inductive and capacitive phase shifts decoupling  $\phi_{E1}$  and  $\phi_B$  flux quanta that comprise the photon. Electric flux quantum propagates to high impedance, matching 25812 ohm quantum Hall and centrifugal impedances at Bohr radius.

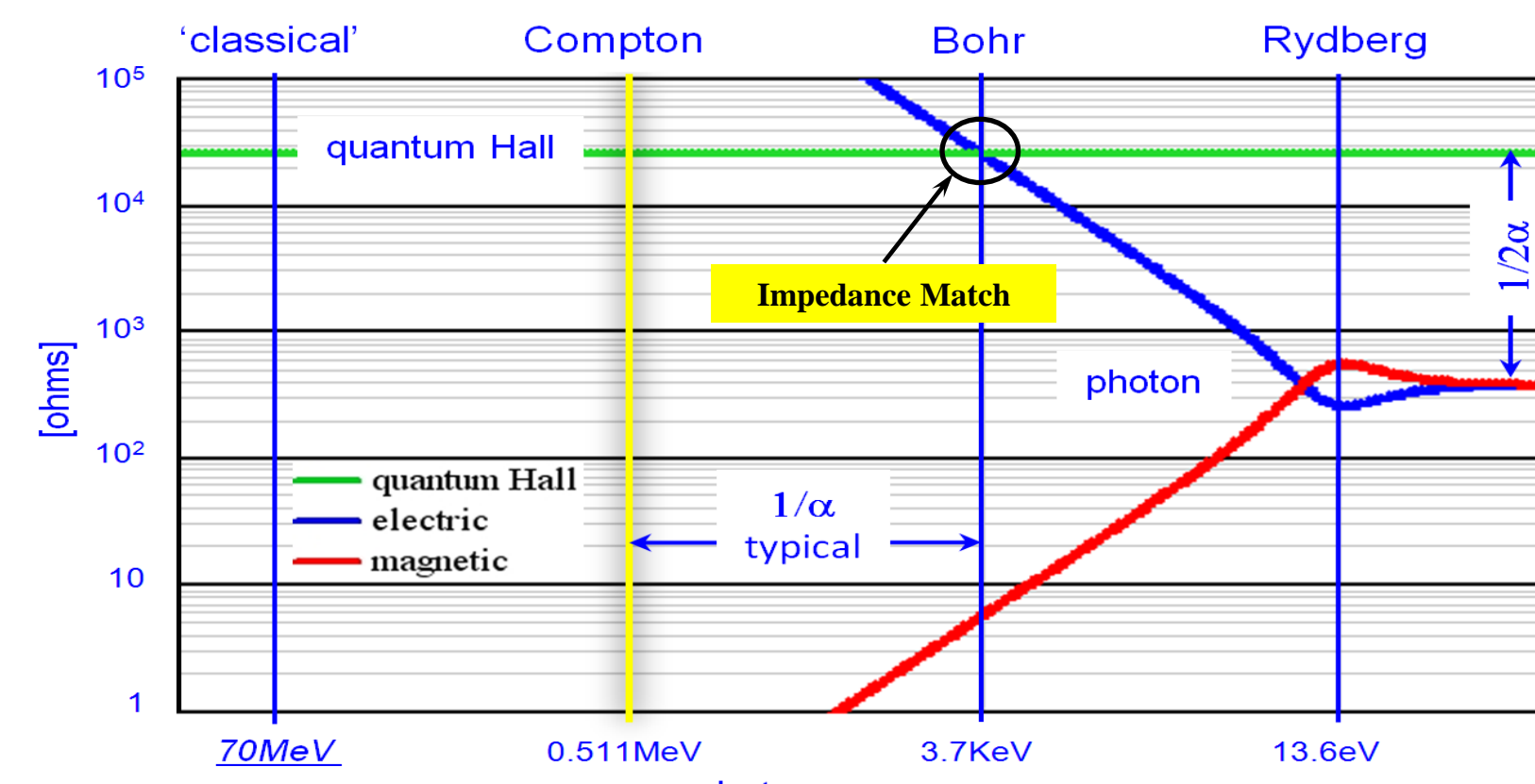


**Fig. 3** Ionization of Hydrogen, Rosetta Stone of atomic physics

### Unstable Particle Spectrum

Impedance quantization extends beyond quantum Hall to impedances associated with all potentials. Figure 4 plots modes indicated by corresponding symbols in figure 2. Green circles connote impedance nodes of W decay at 10 GeV Bottomonium line and 70 MeV platform state. Partial topological symmetry about Compton wavelength with precise impedance matching calculation of  $\pi_0, \eta$ , and  $\eta'$  branching ratios is obvious (blue and red circles), but implications are not yet clear.

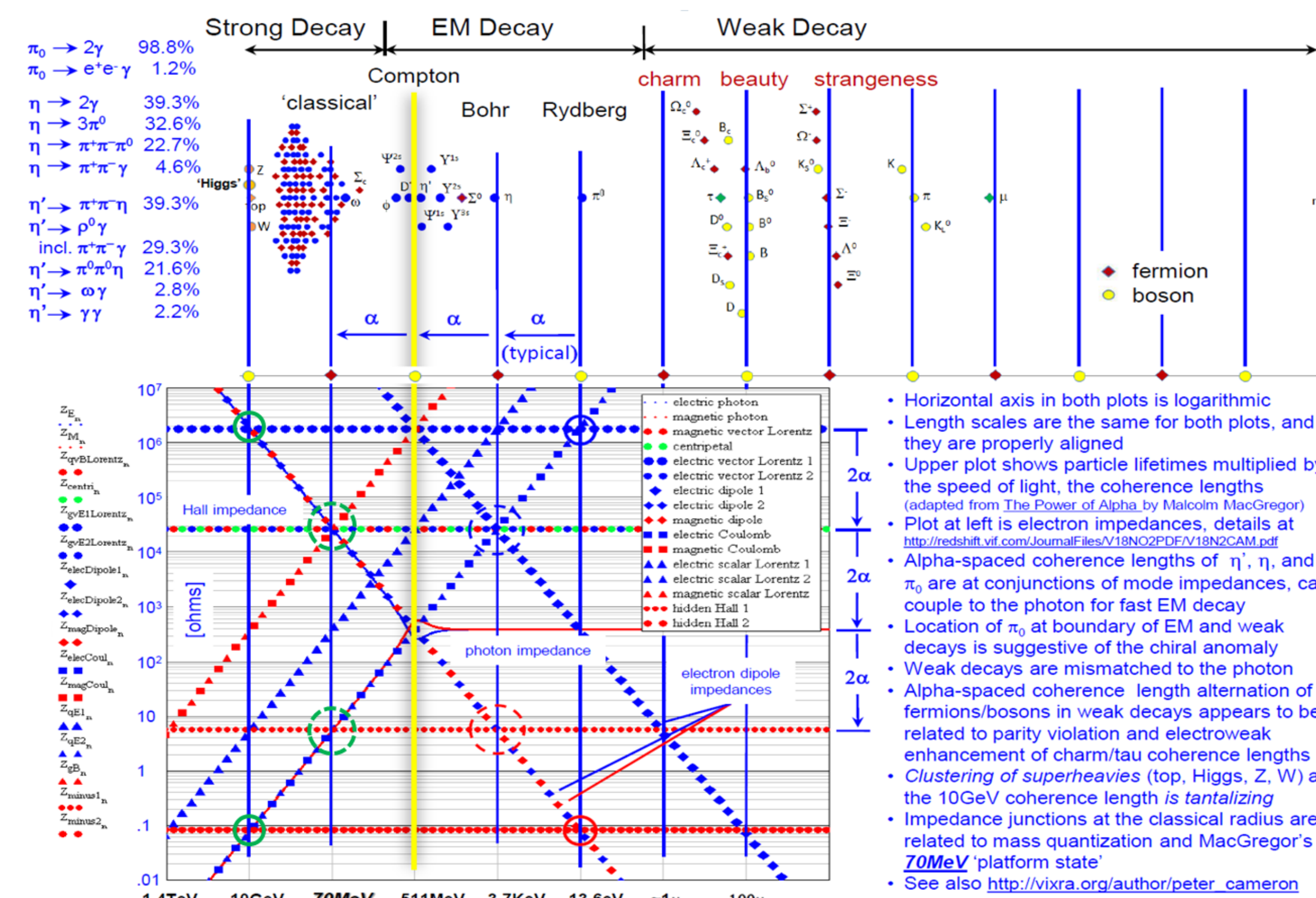


**Fig. 4** Correlation of lifetimes with nodes of the impedance network follows from requirement that impedances be matched for energy transfer. Horizontal scale can be taken to be coherence lengths, quantum phase evolution of S-matrix amplitudes. Of particular interest is muon decay from the  $W$  at the 10 GeV difference mode line.

## Acknowledgments

Many heartfelt thanks to family and friends for support and encouragement, and in particular to Michael Suisse for philosopher's mind, persistently driving the inquiry to the foundations, to the wavefunction.

## 3. Massless Neutrino Oscillation

All experimental data is consistent with massless neutrinos.

Topological duality arises from the difference in coupling to the photon of magnetic and electric charge. With magnetic charge defined by the Dirac relation  $eg = \hbar$  and  $\alpha = e^2/4\pi\epsilon_0\hbar c$ ,  $e \sim \sqrt{\alpha}$  whereas  $g \sim 1/\sqrt{\alpha}$ . The characteristic coherence lengths of figures 3-5 are inverted for magnetic charge. The Compton wavelength  $\lambda = \hbar/mc$  is independent of charge.

With electric charge, fundamental lengths correspond to specific physical mechanisms of photon emission or absorption, matched in both quantized impedance and energy. Inversion results in mismatches in both. The  $\alpha$ -spaced lengths of figures 3-5 correspond to specific physical mechanisms of photon absorption and emission.

Bohr radius cannot be inside Compton wavelength, Rydberg cannot be inside Bohr... specific physical mechanisms of emission and absorption no longer work. Magnetic charge is 'dark', cannot couple to the photon, not despite its great strength, but rather because of it. This topological inversion manifests in swapping of magnetic 'dipole' moment and flux quantum in the two wavefunctions of figure 2. Poles of the flux quantum are at infinity.

In addition to the inversion, there is another topological anomaly. By the Dirac relation  $eg = \hbar$  and SI definition of the magnetic flux quantum  $\phi_0 = \hbar/2e$ , we can write  $\phi_0 = \hbar/2e = g/2$ . Given a factor of two, in SI units vector magnetic flux quantum and trivector magnetic charge are the numerically identical, yet topologically distinct.

The neutrino wavefunction  $\phi_B \phi_{E1} g$  can be thought of as a topological variant on the photon, adding a flux quantum identical to that of the photon, but configured as trivector magnetic charge (the pseudoscalar dual to scalar electric charge), rather than vector magnetic flux quantum. When confined for instance to the electron Compton wavelength, field energy of each of these three wavefunction components is electron rest mass with sub-part-per-billion accuracy.

Flavor is determined by longitudinal field orientation. A consequence of differential phase shifts of magnetic charge relative to photon components, the neutrino 'tumbles' as it propagates.

Associativity limits possible three-body modes. The wavefunction is comprised of vector  $\phi_B$ , bivector  $\phi_{E1}$ , and trivector  $g$  - geometric grades 1, 2, and 3. Applying geometric products to possible mode sequences yields just two that don't contain unphysical negative grades.

$$(3\pm 2)\pm 1 = (5,1)\pm 1 = 6,4,2,0 \quad \text{and} \quad 3\pm(2\pm 1) = 3\pm(3,1) = 6,0,4,2$$

Only products that begin with the largest grade/dimensionality, that begin with pseudoscalar magnetic charge, are physical. This seems most peculiar, given that neutrino oscillations are cyclic. For now we go with the math, in the hope that a plausible physical rationale will eventually present itself. Simplest expedient is to associate the two permitted three-body modes with neutrino and anti-neutrino wavefunctions.

The preliminary conclusion one might draw from this is that the neutrino is not its own antiparticle, is Dirac rather than Majorana. While lacking scalar electric charge, it possesses its own clock, pseudoscalar magnetic charge. One might further conclude that, as in the case of the two-component Dirac spinor, the top and leftmost eight-component wavefunctions of figure 2 are particle and antiparticle in *all* their modes. How do they play with CPT symmetries?

**charge** - reverses orientation of E and B fields of all wavefunction components; in GA these are easily visualized orientable point, line, plane, and volume elements.

**parity** - reverses orientation of basis vectors; again easily visualized, the basis  $e_1, e_2$ , and  $e_3$  of flat Euclidian space.

**time** - reverse relative phases of fields; E leads B or B leads E. Time is the integral of phase.

While of substantial interest to the neutrino community, what motivated this study is the muon collider. Lacking space in the present forum, the hope is that the model presented here fares with CPT will be addressed in detail elsewhere.

The three neutrino two-body modes  $\phi_B \phi_{E1}$ ,  $\phi_B g$ , and  $\phi_{E1} g$  are shown in figures 2 and 4. First of the three  $\phi_B \phi_{E1}$  is the photon, sitting on the skew diagonal, astride the main diagonal. The second  $\phi_B g$  is the magnetic equivalent of the electric scalar Lorentz force, indicated by red triangles in figure 4, and the third  $\phi_{E1} g$  is dual to vector Lorentz force of quantum Hall effect, indicated by scale-invariant solid blue circles at top of figure 4. Given that the only effect of topological impedances such as quantum Hall and Aharonov-Bohm is to shift phases, it seems not unreasonable to expect free space vacuum impedance excited by the neutrino to be identical to the  $\sim 377$  ohms of the photon.

two minute companion video is available at <https://youtu.be/fAtUV10mRVE>